ELECTRON-DEFICIENT PENTAMETHYLCYCLOPENTADIENYL-1,3-BUTADIENE COMPLEXES OF TITANIUM, ZIRCONIUM, AND HAFNIUM

BLENKERS, J; HESSEN, B; VANBOLHUIS, F; WAGNER, AJ; TEUBEN, JH; Bolhuis, Fré van; Wagner, Anton J.

Published in:
Organometallics

DOI:
10.1021/om00146a005

Electron-Deficient Pentamethylcyclopentadienyl–1,3-Butadiene Complexes of Titanium, Zirconium, and Hafnium

Joop Blenkers,[1a] Bart Hessen,[1b] Frê van Bolhuis,[1c] Anton J. Wagner,[1d] and Jan H. Teuben*[1b]

Department of Chemistry, University of Groningen, Nijenborgh 16, 9747 AG Groningen, The Netherlands

Received October 2, 1986

Electron-deficient conjugated diene complexes Cp*M(diene)Cl (M = Ti, Zr, Hf; diene = 2,3-dimethyl-1,3-butadiene, 2-methyl-1,3-butadiene, 1,3-butadiene; Cp* = η-C_5Me_5) were prepared either by reduction of Cp*MCl_3 in the presence of free diene (M = Zr, Hf), by reaction of Cp*$TiCl_3$ with the enediylmagnesium reagent [$Mg(CH_2CMe{=}CMeCH_2)$]·2THF, or through exchange of an η^3-1-methallyl ligand between Cp*M(butadiene)(1-methallyl) and Cp*MCl_3. These 14-electron complexes form 16-electron adducts with a variety of Lewis bases. In all complexes the diene ligand assumes a nonfluxional *s-cis* conformation. NMR spectroscopy indicates that the bonding of the diene ligand has σ^2,π-metallacyclopentene rather than η^4-diene character. EHMO calculations on 14e and 16e model systems point out that on complexation of the Lewis base the metallacyclopentene character should become less pronounced. Both types of compounds were characterized by X-ray analysis. Cp*Hf(C_6H_{10})Cl·C_5H_5N crystallizes in the orthorhombic space group $Pna2_1$ with a = 17.412 (3) Å, b = 8.164 (3) Å, c = 14.837 (3) Å (293 K), and Z = 4. The metallacyclopentene character of the diene ligand is apparent from the Hf–C(diene) distances [Hf–C_T = 2.274 (10)/2.278 (10) Å, Hf–C_C = 2.483 (10)/2.477 (9) Å] and the diene C–C distances [C_C–C_C = 1.384 (15) Å, C_C–C_T = 1.513 (14)/1.493 (14) Å]. Cp*Hf(C_6H_{10})Cl crystallizes in the monoclinic space group C_2 with a = 8.820 (3) Å, b = 12.767 (3) Å, c = 14.486 (3) Å, β = 102.59 (1)° (100 K), and Z = 4. The diene C–C distances [C_C–C_C = 1.400 (12) Å, C_C–C_T = 1.397 (15)/1.525 (13) Å] indicate a large participation of the asymmetric η^3,σ-resonance structure in the bonding of the diene fragment to the metal. The chlorine atom in Cp*M(diene)Cl can easily be substituted to form alkyl, aryl, allyl, and borohydride derivatives. The 14e alkyl complexes show agostic C–H–M interactions in NMR and IR spectra.

Introduction

Several types of conjugated diene complexes of the early transition metals have been synthesized in recent years. These compounds include 18-electron complexes Cp_2M(diene) (M = Zr, Hf),[2] Zr(diene)$_2$(dmpe)·L,[3] and CpM(diene)$_2$ (M = Nb, Ta)[4] and 16-electron complexes (diene)$_2$M(dmpe) (M = Ti, Zr, Hf),[5] CpM(diene)Cl_2 (M = Nb, Ta),[4] and CpM(diene)(allyl) (M = Ti, Zr, Hf).[6,8] Most of these compounds contain diene ligands in an *s-cis* coordination geometry that can best be described as a σ^2,π-metallacyclopentene (Figure 1), in contrast with the η^4-*s-cis*-diene complexes of the later transition metals like (butadiene)$Fe(CO)_3$.[9] Recently extensive reviews on the structure and properties of σ^2,π-metallacyclopentene complexes have been published.[10] Here we wish to report a class of electronically unsaturated 14-electron complexes, Cp*M(diene)Cl, of Ti, Zr, and Hf and their 16-electron Lewis base adducts Cp*M(diene)Cl·L. The effect of the complexation of a Lewis base on the diene structure has been investigated by spectroscopic and X-ray techniques and EHMO calculations. The complexes Cp*M(diene)Cl exhibit interesting structural features and great versatility due to easy substitution of the chlorine ligand. The compounds show an extensive reactivity, of which the reactions with CO have been reported previously.[11]

Results and Discussion

Synthesis. a. Diene Chloride Complexes Cp*M(diene)Cl. Complexes Cp*M(diene)Cl (M = Zr, Hf; diene = 2,3-dimethyl-1,3-butadiene, 2-methyl-1,3-butadiene) were prepared through reduction of Cp*MCl_3 with Na/Hg in THF in the presence of free diene (eq 1). Initial for-

$$\text{Cp*MCl}_3 + \text{Na/Hg} + \text{diene} \xrightarrow{\text{THF}} \text{Cp*M(diene)Cl·THF} \xrightarrow{-\text{THF}} \underset{\mathbf{2,\ 3,\ 5,\ 6}}{\text{Cp*M(diene)Cl}} \quad (1)$$

2, M = Zr, diene = 2-methyl-1,3-butadiene;
3, M = Zr, diene = 2,3-dimethyl-1,3-butadiene;
5, M = Hf, diene = 2-methyl-1,3-butadiene;
6, M = Hf, diene = 2,3-dimethyl-1,3-butadiene

mation of the THF adducts Cp*M(diene)Cl·THF could be observed. THF-free 14e complexes Cp*M(diene)Cl (red for M = Zr, yellow for M = Hf) were obtained through sublimation (diene = C_6H_{10}) or crystallization from toluene (diene = C_5H_8). The Zr complexes were isolated in much lower yields than the Hf analogues, due to oily side products. It has not been possible to isolate products with cyclic dienes such as 1,3-cyclohexadiene and 1,3-cycloheptadiene. This might be caused by steric reasons,

(1) (a) Present address: DSM Research BV, P.O. Box 18, 6160 MD Geleen, The Netherlands. (b) Department of Inorganic Chemistry. (c) Department of Molecular Structure. (d) Department of Chemical Physics.

(2) (a) Erker, G.; Wicher, J.; Engel, K.; Rosenfeld, F.; Dietrich, W.; Krüger, C. *J. Am. Chem. Soc.* **1980**, *102*, 6344. (b) Yasuda, H.; Kajihara, Y.; Mashima, K.; Nagasuna, K.; Lee, K.; Nakamura, A. *Organometallics* **1982**, *1*, 388. (c) Erker, G.; Wicher, J.; Engel, K.; Krüger, C. *Chem. Ber.* **1982**, *115*, 3300. (d) Erker, G.; Wicher, J.; Krüger, C.; Chiang, A. P. *Ibid.* **1982**, *115*, 3311.

(3) (a) Datta, S.; Wreford, S. S.; McNeese, T. J. *J. Am. Chem. Soc.* **1979**, *101*, 1053. (b) Datta, S.; Fischer, M. B.; Wreford, S. S. *J. Organomet. Chem.* **1980**, *188*, 353.

(4) Yasuda, H.; Tatsumi, K.; Okamoto, T.; Mashima, K.; Lee, K.; Nakamura, A.; Kai, Y.; Kanehisa, N.; Kasai, N. *J. Am. Chem. Soc.* **1985**, *107*, 2410.

(5) Wreford, S. S.; Whitney, J. F. *Inorg. Chem.* **1981**, *20*, 3918.

(6) Zwijnenburg, A.; Van Oven, H. O.; Groenenboom, C. J.; De Liefde Meijer, H. J. *J. Organomet. Chem.* **1975**, *94*, 23.

(7) (a) Blenkers, J.; De Liefde Meijer, H. J.; Teuben, J. H. *Recl. Trav. Chim. Pays-Bas* **1980**, *99*, 216. (b) Blenkers, J.; De Liefde Meijer, H. J.; Teuben, J. H. *J. Organomet. Chem.* **1981**, *218*, 383.

(8) Erker, G.; Berg, K.; Krüger, C.; Müller, G.; Angermund, K.; Benn, R.; Schroth, G. *Angew. Chem.* **1984**, *96*, 445.

(9) Mills, O. S.; Robinson, G. *Proc. Chem. Soc.* **1960**, 421.

(10) (a) Yasuda, H.; Tatsumi, K.; Nakamura, A. *Acc. Chem. Res.* **1985**, *18*, 120. (b) Erker, G.; Krüger, C.; Müller, G. *Adv. Organomet. Chem.* **1985**, *24*, 1.

(11) Blenkers, J.; De Liefde Meijer, H. J.; Teuben, J. H. *Organometallics* **1983**, *2*, 1483.

(12) Smith, G. M.; Suzuki, H.; Sonnenberger, D. C.; Day, V. W.; Marks, T. J. *Organometallics* **1986**, *5*, 549.

0276-7333/87/2306-0459$01.50/0

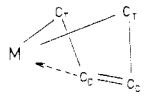

Figure 1. σ^2,π-Metallacyclopentene bonding mode in a diene–metal complex (C_T = terminal diene carbon; C_C = central diene carbon).

possibly due to a preferred "supine" (i.e., with the terminal diene carbons C_T directed toward the Cp* group) coordination of the diene, as in $CpM(diene)Cl_2$ (M = Nb, Ta),[4] in which case the hydrocarbon group bridging the diene carbons would interfere with the Cp* methyl groups. A notable exception is $Cp^*Zr(\eta^4\text{-}C_8H_8)(\eta^3\text{-}C_3H_5)$ which contains a "prone" coordinated η^4-cyclooctatetraene ligand.[13]

The reductive procedure was unsuccessful for M = Ti. Reduction of Cp^*TiCl_3 did take place, but no complexation of the diene to the metal could be observed. Cp*Ti(2,3-dimethyl-1,3-butadiene)Cl (**7**) was obtained through reaction of Cp^*TiCl_3 with (2,3-dimethyl-2-butene-1,4-diyl)-Mg·2THF in THF at 0 °C. After pentane extraction the blue-green THF-free 14e complex can be directly obtained in moderate yield.[14]

As the reductive procedure was also unsuccessful for the preparation of complexes with unsubstituted butadiene, an alternative method was used, utilizing the butadiene ligand already present in the complexes $Cp^*M(\eta^4\text{-}C_4H_6)(\eta^3\text{-}C_4H_7)$ (M = Ti, Zr, Hf).[7] Upon mixing these complexes with Cp^*MCl_3 in diethyl ether ligand exchange occurred (eq 2). A similar exchange reaction between

$$Cp^*MCl_3 + Cp^*M(C_4H_6)(C_4H_7) \xrightarrow{Et_2O} \underset{1,4}{Cp^*M(C_4H_6)Cl} + Cp^*M(C_4H_7)Cl_2 \quad (2)$$

M = Zr, 1; M = Hf, 4

$CpZrCl_3$ and $CpZr(C_3H_5)_3$ was recently reported.[8] Remarkable differences between Ti, Zr, and Hf were noticed in this reaction: for M = Zr the reaction proceeded smoothly (though slowly) according to eq 2, in which purple **1** precipitated from the solution and yellow $Cp^*Zr(C_4H_7)Cl_2$ could subsequently be crystallized from the reaction liquid.[15] For M = Hf the precipitated orange-brown crystals showed a stoichiometry of $C_{26}H_{36}Cl_4Hf_2$ (elemental analysis). This compound can probably best be described as $Cp^*Hf(C_4H_6)(\mu\text{-}Cl)_2HfCl_2Cp^*$, an adduct of **4** with Cp^*HfCl_3. In THF the compound is broken up into $Cp^*Hf(C_4H_6)Cl$·THF and Cp^*HfCl_3·2THF (NMR), which were inseparable. For M = Ti the reaction probably takes place according to eq 2, but the produced $Cp^*Ti(C_4H_7)Cl_2$ is unstable at room temperature and decomposes to green insoluble Cp^*TiCl_2,[16] which forms an inseparable mixture with the greenish-blue $Cp^*Ti(C_4H_6)Cl$.

(13) Highcock, J. W.; Mills, R. M.; Spencer, J. L.; Woodward, P. *J. Chem. Soc., Chem. Commun.* **1982**, 128.

(14) (2-Butene-1,4-diyl)magnesium reagents did not prove useful in synthesizing the corresponding Zr and Hf compounds as products are formed that are poorly soluble in hydrocarbon solvents. The diene appears to be coordinated to the metal (NMR), but the products are probably dimeric or oligomeric due to complexation of $MgCl_2$ (elemental analysis). These complexed salts could not be removed through treatment with 1,4-dioxane.

(15) The compounds $Cp^*M(C_4H_7)Cl_2$ (M = Zr, Hf) show an IR absorption characteristic for an η^3-1-methallyl group at 1562 and 1560 cm^{-1} for M = Zr and Hf, respectively. These frequencies are 28 cm^{-1} higher than in the corresponding $Cp^*M(C_4H_6)(C_4H_7)$ complexes,[7] due to the electron-withdrawing Cl ligands.

(16) Ti–Cl vibration at 440 cm^{-1} and Cp* vibrations in the IR spectra identical with those of Cp^*TiCl_2 described in ref 17.

(17) Nieman, J.; Pattiasina, J. W.; Teuben, J. H. *J. Organomet. Chem.* **1984**, *262*, 157.

Table I. Thermal Properties of the Compounds Cp*M(diene)X[a]

compd	mp	decomp temp	compd	mp	decomp temp
2	176	*b*	**9**	72	131
3	125	134	**10**	70	104
5	144	151	**11**	114	155
6	114	140	**12**	76	182
7	127	110–130[c]	**13**	114	244
			14	88	220

[a] Melting point and decomposition temperatures in degree Celcius, determined by DTA. [b] Decomposes while melting. [c] Very broad exothermic effect.

The difference in behavior of Hf vs. Zr in this reaction is not fully understood but may be related to differences in Lewis acidity.

Complexes Cp*M(diene)Cl are very air sensitive but thermally quite stable (Table I). Their solubility is very much dependent on the degree of substitution of the diene. Thus the C_6H_{10} complexes are soluble in all common hydrocarbon solvents, the C_5H_8 complexes only sparingly soluble in aromatic solvents, and the C_4H_6 complexes hardly soluble at all. All Zr and Hf complexes form soluble adducts in THF. The 14e complexes were characterized by spectroscopic methods (NMR, IR) and elemental analysis. The monomeric nature of $Cp^*M(C_6H_{10})Cl$ was demonstrated by cryoscopy in benzene for **3** and confirmed in the solid state by X-ray diffraction on **6** (vide infra).

All compounds show the characteristic η^5-Cp* absorptions in the IR spectrum around 2710, 1490, 1420, 1370, 1060, 1020, 800, and 590 cm^{-1}.[18] Vibrations (ν_{CC}) of the complexed conjugated dienes are found between 1550 and 1350 cm^{-1} and are in agreement with data from other diene complexes, both of the early[2b] and late transition metals.[19] However, the assignment is difficult due to the partial coincidence with the Cp* absorptions near 1500 cm^{-1}. Reaction of the diene chloride complexes with dry oxygen results in the quantitative release of the coordinated diene.

b. Lewis Base Adducts Cp*M(diene)Cl·L. Lewis base adducts Cp*M(diene)Cl·L (M = Zr, Hf) are easily formed by adding free ligand (pyridine, THF, RCN, PR_3, $P(OR)_3$) to hydrocarbon solutions of the 14e complexes. Depending on the solubility of the resultant adducts, they can be recrystallized from diethyl ether or pentane. For the Ti complex **7** no adduct formation was observed (with the exception of *t*-BuCN, but this adduct could not be isolated due to subsequent fast reaction[20]), probably for steric reasons. The stability of the THF adducts varies with the degree of substitution of the diene: complexes of mono- and nonsubstituted dienes lose coordinated THF readily under vacuum at room temperature, while the C_6H_{10} complexes **3** and **6** can only be freed from THF through vacuum sublimation. The adducts $Cp^*M(C_6H_{10})Cl\cdot L$ (M = Zr, L = PMe_3; M = Hf, L = pyridine, 2,6-xylyl cyanide, THF, PMe_3, $P(OMe)_3$) were characterized by spectroscopic methods (IR, NMR) and elemental analysis. No formation of PPh_3 adducts has been found, probably due to steric reasons. Reaction of **6** with 0.5 mol of the diphosphine dmpe yields $[Cp^*Hf(C_6H_{10})Cl]_2$ dmpe, with the dmpe ligand bridging the two Hf centers.[21] The

(18) Bercaw, J. E. *J. Am. Chem. Soc.* **1974**, *96*, 5087.

(19) Fischer, E. O.; Werner, H. *Metal π-complexes*; Elsevier Publishing Company: Amsterdam, London, New York, 1966; Vol. 1.

(20) Hessen, B.; Blenkers, J.; Teuben, J. H., to be submitted for publication.

(21) $[Cp^*Hf(C_6H_{10})Cl]_2$·dmpe: ^1H NMR (C_6D_6, 200 MHz) 2.28 (s, 12 H, diene CH_3), 2.06 (s, 30 H, Cp*), 1.41 (m, 4 H, PCH_2–), 1.00 (d, 8.9 Hz, 4 H, *syn*-CH_2), 0.86 (m, 12 H, PMe), −0.05 ppm (d, 8.9 Hz, 4 H, *anti*-CH_2). Anal. Calcd for $C_{38}H_{66}Hf_2Cl_2P_2$: C, 45.07; H, 6.57; Cl, 7.00. Found: C, 44.42; H, 6.70; Cl, 6.95.

Table II. Borohydride IR Absorption Frequencies (in cm^{-1}) in $Cp^*Hf(C_6H_{10})(\eta^2\text{-}BH_4)(L)$

L	ν(B–H) terminal	ν(B–H) bridging	$\nu(BH_4)$ deformation
	2450, 2410	2100, 2025, 1965	1121
pyridine	2415, 2385	2235, 2190, 2150	1120
PMe_3	2410, 2375	2225, 2150, 2120	1122

adduct formation step is very important in the reactivity of the 14e complexes toward unsaturated molecules with electron lone pairs (e.g., CO,[11] RNC,[22] RCN, and R_2CO[20]).

c. Hydrocarbon and Borohydride Derivatives. The chlorine ligand in the complexes Cp*M(diene)Cl can be easily replaced by a hydrocarbon group through reaction with 1 mol of the appropriate Grignard or alkyllithium reagent in diethyl ether at −30 °C.[23] Only the 2,3-dimethyl-1,3-butadiene complexes $Cp^*M(C_6H_{10})R$ (M = Ti, R = Me (**8**); M = Hf, R = Me (**9**), Et (**10**), neopentyl (**11**), Ph (**12**), η^3-allyl (**13**), η^3-1-methallyl (**14**)) are described here. These complexes are thermally stable in the solid state at room temperature (Table I).

In solution the alkyl compounds are considerably less stable. Thermal decomposition of **9** in benzene at 40 °C yields methane (0.8 mol/Hf) and small amounts of ethane, propane, and butane (<0.2 mol/Hf). The major decomposition pathway, leading to methane, probably proceeds via hydrogen abstraction from the solvent or the methyl groups of the Cp* ligand.[25] Formation of small amounts of C_2–C_4 hydrocarbons makes partial decomposition via homolytic fission of the Hf–CH_3 bond with formation of methyl radicals likely. Thermal decomposition of **10** in benzene at room temperature yields ethane (0.95 mol/Hf), ethene (0.01 mol/Hf), and traces of propane, indicating that under these circumstances proton abstraction from the solvent or the Cp* group is preferred above β-H elimination.

In the IR spectrum of **10** there is an indication for a β-agostic C–H–M interaction;[26a] three C–H stretch vibrations are visible at 2600, 2500, and 2440 cm^{-1}, substantially lower than normal ethyl C–H stretch vibrations (3000–2850 cm^{-1}).[27] Further evidence for agostic behavior in the complexes $Cp^*Hf(C_6H_{10})R$ is presented by the NMR spectra (vide infra).

Compounds **13** and **14** show characteristic IR absorptions for an η^3-bound allylic ligand: ν_{CC} = 1499 and 1533 cm^{-1} respectively. The latter absorption represents an η^3-1-methallyl group with the methyl substituent in a syn position, corresponding to the bonding of the ligand in $Cp^*Hf(C_4H_6)(C_4H_7)$[7] and $Cp_2Ti(C_4H_7)$.[28]

The alkyl derivatives do not form Lewis base adducts as easily as the chloride complexes (no adduct formation with PEt_3 was observed, probably due to steric reasons), but the adduct $Cp^*Hf(C_6H_{10})CH_3$·py was characterized by NMR.[29a]

Table III. ^1H NMR Data for $Cp^*M(C_6H_{10})Cl$[a]

complexes	Cp*	=CH_2 syn	=CH_2 anti	$\lvert^2J_{HH}\rvert$	diene–Me
3	1.96	2.40	0.55	9.5	2.0
6	2.01	2.14	0.01	11.0	2.08
7	1.84	2.69	1.35	8.7	1.85

[a] Data recorded at 200 MHz in C_6D_6 at 20 °C; shifts in ppm relative to Me_4Si and coupling constants in Hz.

Table IV. ^{13}C NMR Data for $Cp^*M(C_6H_{10})Cl$[a,b]

complexes	=C(R)—	=CH_2	diene–Me
3	131.0 (s)	67.2 (dd, 132, 148)	23.5 (q, 125)
6	128.6 (s)	67.7 (dd, 131, 149)	23.2 (q, 127)
7	136.1 (s)	82.1 (t, 147)	23.8 (q, 125)

[a] Data recorded at 50.3 MHz in C_6D_6 at 20 °C; shifts in ppm relative to Me_4Si and coupling constants in Hz. [b] C_5Me_5 varies from 119.8 (**6**) to 122.3 ppm (**7**) and $C_5(CH_3)_5$ from 11.5 to 12.0 ppm (q, 127 Hz).

Reaction of **6** with $NaBH_4$ in diethyl ether gives smooth formation of the borohydride derivative $Cp^*Hf(C_6H_{10})BH_4$. IR spectroscopy shows that the compound contains an η^2-BH_4 group.[30] Absorption wavenumbers are given in Table II. Attempts to synthesize a butadiene–hydrido complex (of interest because of the possibility of conversion to a methallyl complex, the inverse of the process described for the formation of $Cp^*M(C_4H_6)(C_4H_7)$ from $Cp^*M(C_4H_7)_3$ (M = Ti, Zr, Hf)[7]), by abstraction of BH_3 from the borohydride complex with Lewis bases like pyridine, NEt_3, PMe_3, and TMEDA, failed. With pyridine and PMe_3 stable adducts $Cp^*Hf(C_6H_{10})BH_4$·L were formed.[29b] IR spectroscopy showed that the BH_4 group is still η^2-bonded and that the Hf(μ-H)$_2$B bonding has been strengthened by the coordination of the Lewis base, as reflected in the increased wavenumbers for the vibrations of the Hf(μ-H)$_2$B bridge (Table II). Tertiary amines did not form adducts, but even after the mixture was stirred in toluene at 60 °C for days, high yields of the starting material could be recovered.

NMR Studies. a. The Diene Fragment. ^1H- and ^{13}C-NMR data for the compounds Cp*M(diene)Cl and Cp*(diene)Cl·L are presented in the Tables III–VI. The diene resonances show several features typical for conjugated dienes, *s-cis* coordinated to an early transition metal[2a,b,d,4] and possessing a distinct σ^2,π-metallacyclopentene character: the relatively large geminal coupling constants $\lvert^2J_{HH}\rvert$ of the diene methylene groups (7.0–11.5 Hz vs. 2.4 Hz in $(\eta^4\text{-}C_4H_6)Fe(CO)_3$[31]) and $^1J_{CH}$ coupling constants that are considerably smaller than the usual values for sp^2-hybridized carbon atoms (131–149 Hz vs. 155–160 Hz) suggest a considerable amount of rehybridization of the diene methylene groups toward sp^3 hybridization. The marked downfield shift of the olefinic protons in the non-2,3-disubstituted diene complexes (5.8–6.0 ppm) is a characteristic of *s-cis* coordinated diene ligands.[4,32] The upfield shift of the diene methylene protons in the 14e complexes upon going down the group from Ti to Hf is accompanied by an increase of the geminal coupling constant between the syn and anti methylene

(22) Blenkers, J. Ph.D. Thesis, University of Groningen, 1982.
(23) Reaction of **6** with 2 mol of MeMgI in diethyl ether yields an as yet not fully characterized organo Hf compound, possibly of the nature of $[Cp^*Hf(C_6H_{10})Me]_2MgMe_2$, which is very active in the polymerization of 2-vinylpyridine to highly isotactic poly(2-vinylpyridine).[24]
(24) Meijer-Veldman, M. E. E.; Tan, Y. Y.; De Liefde Meijer, H. J. *Polymer Commun.* **1985**, *26*, 200.
(25) (a) Bercaw, J. E.; Marvich, R. H.; Bell, L. G.; Brintzinger, H. H. *J. Am. Chem. Soc.* **1972**, *94*, 1219. (b) Pattiasina, J. W.; Hissink, C. E.; De Boer, J. L.; Meetsma, A.; Teuben, J. H.; Spek, A. L. *Ibid.* **1985**, *107*, 7758.
(26) (a) Brookhart, M.; Green, M. L. H. *J. Organomet. Chem.* **1983**, *250*, 395. (b) Den Haan, K. H.; Teuben, J. H. *Recl. Trav. Chim. Pays-Bas* **1984**, *103*, 333.
(27) Maslowski, E., Jr. *Vibrational Spectra of Organometallic Compounds*; Wiley: New York, London, Sydney, Toronto, 1977.
(28) Martin, H. A.; Jellinek, F. *J. Organomet. Chem.* **1967**, *8*, 115.
(29) (a) $Cp^*Hf(C_6H_{10})CH_3$·py; ^1H NMR (C_6D_6, 200 MHz) 2.10 (s, 21 H, Cp* + diene CH_3), 0.92 (d, 7.1 Hz, 2 H, *syn*-CH_2), 0.25 (d, 7.1 Hz, 2 H, *anti*-CH_2), −0.24 (s, 3 H, $HfCH_3$), 8.6, 7.1, 6.8 ppm (m, pyridine). (b) $Cp^*Hf(C_6H_{10})BH_4$·py: ^1H NMR (C_6D_6, 60 MHz) 1.98 (s, 15 H, Cp*), 1.77 (s, 6 H, diene CH_3), 0.90 (d, 7 Hz, 2 H, *syn*-CH_2), 0.57 ppm (d, 7 Hz, 2 H, *anti*-CH_2).
(30) Marks, T. J.; Kolb, J. R. *Chem. Rev.* **1977**, *77*, 263.
(31) (a) Bachmann, K.; Von Philipsborn, W. *Org. Magn. Reson.* **1976**, *8*, 648. (b) Ruh, S.; Von Philipsborn, W. *J. Organomet. Chem.* **1977**, *127*, C59.
(32) Benn, R.; Schroth, G. *J. Organomet. Chem.* **1982**, *228*, 71.

Table V. ^{1}H NMR Data for Cp*M(diene)Cl•L[a,b]

complex	L	=CH—	=CH$_2$ syn	=CH$_2$ anti	$\|^2J_{HH}\|$	Me	L
1[d]	THF-d_8	6.02 (m)	1.49 (m)	0.62 (m)			
2[d]	THF-d_8	5.54 (t, 7.5)	1.2 (m)	0.5 (m)		2.0[c]	
3[d]	THF-d_8		1.14 (d)	0.62 (d)	7.1	2.09	
3[f]	PMe_3		1.12 (d)	0.24 (d)	7.6	2.16	0.33 (d, 5.4)
4[d]	THF-d_8	6.01 (m)	1.19 (m)	0.17 (m)			
5[d]	THF-d_8	5.55 (t, 7.5)	1.2 (m)	0.3 (m)		2.42	
6[f]	XCN[g]		0.97 (d)	0.40 (d)	7.4	2.19	6.5–7.0 (m, 3 H), 2.36 (s, 6 H)
6[f]	py		1.02 (d)	0.41 (d)	7.3	1.9 (br)	6.4 (m, 2 H), 6.7 (m, 1 H), 8.7 (m, 2 H)
6[e]	THF		1.2[c]	0.37 (d)	7.5	2.20	1.23 (m, 4 H), 3.49 (m, 4 H)
6[e]	PMe_3		0.81[c]	−0.12 (d)	8.8	2.21	0.83 (d, 5.8)
6[e]	$P(OMe)_3$		1.50 (d)	0.03 (d)	9.5	2.28	3.24 (d, 10.3)

[a] Data recorded at 200 MHz and 20 °C; shifts in ppm relative to Me_4Si and coupling constants in Hz. [b] Cp* resonances around 2.0 ppm. [c] Overlapped (partly) by other resonances. [d] In THF-d_8. [e] In benzene-d_6. [f] In toluene-d_8. [g] XCN is 2,6-xylyl cyanide.

Table VI. ^{13}C NMR Data for Cp*M(diene)Cl•L[a,b]

complex	L	=C(R)—	=CH$_2$	Me	L
1[c]	THF-d_8	123.3 (d, 164)	56.5 (t, 142)		
2[c]	THF-d_8	134.1 (s), 119.2 (d, 162)	60.5 (t, 138), 55.6 (t, 138)	25.8 (q, 126)	
3[e]	PMe_3	125.1 (s)	63.6 (t, 139)	24.4 (q, 126)	15.8 (dq, 15, 126)
4[c]	THF-d_8	122.2 (d, 160)	54.2 (t, 139)		
5[c]	THF-d_8	134.0 (s), 118.5 (d, 160)	54.7 (t, 138), 59.6 (t, 138)	26.4 (q, 126)	
6[d]	py	125.5 (s)	61.3 (t, 137)	21.7 (q, 125)	151.5 (d, 183), 123.8 (dt, 7, 166), 138.0 (d, 167)
6[d]	THF	127.1 (s)	63.8 (t, 139)	22.7 (q, 124)	26.0 (t, 135), 73.9 (t, 151)
6[d]	PMe_3	122.7 (s)	60.8 (t, 139)	23.1 (q, 126)	14.7 (dq, 15, 134)
6[d]	$P(OMe)_3$	125.6 (s)	64.3 (t, 138)	22.9 (q, 126)	50.4 (q, 146)

[a] Data recorded at 50.3 MHz and 20 °C; shifts in ppm relative to Me_4Si and coupling constants in Hz. [b] C_5Me_5 varies from 118.4 to 120.6 ppm and $C_5(CH_3)_5$ from 11.4 to 11.9 ppm. [c] In THF-d_8. [d] In benzene-d_6. [e] In toluene-d_8.

protons. This effect has been observed before in the complexes $(C_8H_8)M(C_4H_6)$[32] and can probably be ascribed to an increase in σ-contribution to the diene–metal bonding in the sequence Ti < Zr < Hf. This is in line with recent structural observations in the Cp_2M(diene) system.[33]

In marked contrast to most other group 4 metal–diene complexes like Cp_2M(diene)[2b,d,32] and $(C_8H_8)M$(diene),[32] the diene fragment in Cp*M(diene)Cl and its Lewis base adducts shows no fluxional behavior in the NMR spectra even up to 100 °C. A similar rigidity is exhibited by the diene in the complexes $CpM(diene)Cl_2$ (M = Nb, Ta),[4] which are isoelectronic with the Lewis base adducts Cp*M(diene)Cl·L (M = Zr, Hf).

Remarkable differences are seen in the NMR spectra between the 14e and 16e complexes. Upon complexation of the Lewis base the difference in chemical shift between the methylene protons syn and anti to the 2,3-substituents decreases from 2 to 0.5–0.9 ppm, mainly due to an upfield shift of 1.0–1.4 ppm of the syn protons. This seems to be a good probe for the formation of 16e complexes Cp*M(diene)R·L, e.g., in reaction mixtures. This shift of the syn protons is accompanied by a decrease in $|^2J_{HH}|$. There appears to be a trend of increasing $|^2J_{HH}|$ in the adducts with increasing π-acceptor and decreasing σ-donor abilities of the Lewis base. Possibly the decrease in $|^2J_{HH}|$ can be related to a less pronounced σ^2,π-character of the diene in the 16e adducts. Comparison of the ^{13}C NMR spectra on this point is not so easy, as the 14e and 16e complexes show different methylene carbon multiplicities. The methylene carbons in the Zr and Hf 14e complexes exhibit a double doublet coupling pattern, contrary to the 16e complexes (and most other *cis*-diene group 4/5 transition-metal complexes[2,4]) which show a triplet. Although to be expected for methylene groups with two protons with different magnetical environment, a double doublet has so far only been observed for Cp^*_2Th(*s-cis*-diene) at the slow-exchange limit[12] and *trans*-diene complexes like Cp_2Zr(*s-trans*-C_4H_6).[2c] When an averaged value was used for $^1J_{CH}$, no clear trend is visible. A comparison of diene coordination geometry and bonding in the 14e and 16e systems has been made by extended Hückel MO calculations (vide infra).

At room temperature all complexes of symmetrically substituted dienes give spectra indicating a mirror plane in the complex through the metal, bissecting the central diene C–C bond. For steric reasons it is unlikely that the 16e adducts have a coordination geometry with a mirror plane. Indeed, upon lowering the temperature the interconversion of the two configurations, depicted below, becomes slow on the NMR time scale, and the two halves of the diene show different chemical environments.

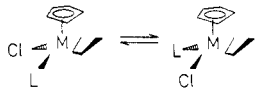

For example the NMR spectra of $Cp^*Hf(C_6H_{10})Cl$·py at the high- and low-temperature limits (toluene-d_8, 200 MHz) show the following diene resonances (δ):

T, °C	Me	CH$_2$ syn	CH$_2$ anti
60	1.88	1.02	0.41
−45	1.32	1.36	0.50
	2.56	0.78	0.42

From the coalescence of the methyl resonances (T_c = 15 ± 2 °C) the $\Delta G^\ddagger$ for the interconversion at T_c was estimated to be 13.2 (± 0.1) kcal mol^{-1}. The difference in chemical shift for the two diene methyl groups in the pyridine adduct ($\Delta\delta$ = 1.24 ppm) is very large compared to complexes of other Lewis bases (e.g., $Cp^*Zr(C_6H_{10})$-Cl·PMe_3 (toluene-d_8, −75 °C): δ_{Me} 2.03, 2.14; $\Delta\delta$ = 0.11 ppm). The large upfield shift for one of the methyl groups is probably due to the π-system of the pyridine ligand, which, as can be seen in the X-ray structure (vide infra), is well-positioned to have a shielding influence on the

(33) Krüger, C.; Müller, G.; Erker, G.; Dorf, U.; Engel, K. *Organometallics* **1985**, *4*, 215.

Table VII. ^{1}H NMR Data for Cp*M(C_6H_{10})R[a]

	=CH_2				R[d]			
complex	syn	anti	$\|^2J_{HH}\|$	diene–Me	α	β	γ	δ
8	2.67	0.95	8.5	2.07	−0.10 (s)			
9	2.0[b]	−0.28	10.8	2.10	−0.72 (s)			
10	1.82	−0.04	10.5	2.09	−0.47 (q, 7.0)	−0.05 (t, 7.0)		
11	1.86	−0.38	11.5	2.32	−0.38 (s)		0.90 (s)	
12	2.25	0.12	11.0	1.77		6.7 (m, 2 H)	7.15 (m, 3 H)	
13[c]	1.84	−0.82	8.5	2.0[b]	1.3 (m, 2 H)	5.7 (m, 1 H)	1.3 (m, 2 H)	
14	2.0[b]	−0.89	8.5	2.13	1.2 (m, 2 H)	5.68 (dt, 11.0, 14.0)	1.2 (m, 1 H)	1.52 (d, 6.0, 3 H)

[a] Data recorded at 200 MHz in C_6D_6 at 20 °C except where stated otherwise; chemical shifts in ppm relative to Me_4Si and coupling constants in Hz. All Cp* resonances around 2.0 ppm. [b] Partly overlapped by the Cp* resonance. [c] In toluene-d_8. [d] For **13** and **14**: $CH_{\alpha 2}$–CH_β–CH_γ–Me_δ.

Table VIII. ^{13}C NMR Data for Cp*Hf(C_6H_{10})R[a]

				R[d]			
complex	=C(Me)—	=CH_2	diene–Me	α	β	γ	δ
9	126.3 (s)	68.5 (dd, 131, 146)	23.4 (q, 125)	54.0 (q, 112)			
10	123.8 (s)	61.1 (dd, 131, 147)	23.6 (q, 127)	47.0 (t, 131)	0.0 (q, 121)		
11	125.9 (s)	68.9 (dd, 131, 146)	25.0 (q, 127)	89.3 (t, 104)	36.5 (s)	35.9 (q, 123)	
12	128.4 (s)	68.2 (dd, 130, 149)	24.2 (q, 127)	189.4 (s)	127.5 (d, 155)	127.2 (d, 155)	126.5 (d, 155)
13[b]	117.7 (s)	53.6 (t, 143)	22.8 (q, 125)	60.3 (t, 150)	129.6 (d, 153)	60.3 (t, 150)	
14[c]	117.3 (s)	54.8 (t, 141)	23.5 (q, 127)	52.5 (t, 148)	129.9 (d, 155)	79.6 (d, 141)	16.2 (q, 127)

[a] Data recorded at 50.3 MHz in C_6D_6 at 20 °C unless stated otherwise; chemical shifts in ppm relative to Me_4Si and coupling constants in Hz. [b] In toluene-d_8. [c] Recorded at 70 °C. [d] For **13** and **14**: $CH_{\alpha 2}$–CH_β–CH_γ–Me_δ. [e] C_5Me_5 varies from 116.5 to 118.6 ppm and $C_5(CH_3)_5$ from 11.3 to 12.8 ppm (q, 126 Hz).

above lying methyl group. In the room-temperature ^{13}C NMR spectrum of Cp*Hf(C_6H_{10})Cl·py this interconversion caused considerable broadening of the diene carbon signals. The interconversion appears to be a unimolecular process: the amount of coalescence at various temperatures for Cp*Hf(C_6H_{10})Cl·py did not change upon adding free pyridine (3 equiv) to the solution.

In the 1-methallyl complex **13** a similar phenomenon occurs due to a fast η^3–η^1 dynamic process of the η^3-1-methallyl group. The behavior is similar to the process described for Cp*M(η^4-C_4H_6)(η^3-C_4H_7) (M = Ti, Zr, Hf).[7b]

b. Other Metal-Bonded Hydrocarbon Groups. The ^{1}H and ^{13}C-NMR data for the compounds Cp*M(C_6H_{10})R are presented in Tables VII and VIII. In the ^{13}C NMR spectra of the 14e alkyl derivatives the α-carbons are found at considerably lower field than in the corresponding parent hydrocarbons. Furthermore there are strong indications that these electronically very unsaturated alkyl complexes show agostic C–H–M interactions. In the methyl (**9**) and neopentyl (**11**) Hf complexes the $^1J_{CH}$ coupling constants on the α-carbons are significantly lower than the usual 125 Hz for an sp^3-hybridized carbon atom. In a fluxional agostic system one expects the $^1J_{CH}$ to be an averaged value:[26a] **9**, $^1J_{CH}$(obsd) = 112 Hz = (2 × 125 + 1 × 86)/3 Hz; **11**, $^1J_{CH}$(obsd) = 104 Hz = (1 × 125 + 1 × 83)/2 Hz. The $^1J_{CH}$ values thus calculated for the agostic hydrogen in the static form for **9** and **11** (86 and 83 Hz, respectively) are in reasonable agreement with values found in agostic alkyl complexes with only one α-hydrogen (e.g., Cp*$_2$YCH($SiMe_3$)$_2$, $^1J_{CH}$ = 84.2 Hz[26b]). In the corresponding ethyl complex **10** the α-agostic interaction is replaced by a β-agostic interaction: the $^1J_{CH}$ on the α-carbon (131 Hz) is now larger than usual, reflecting an increased sp^2 character of the α-carbon, while the β-carbon resonance is shifted to high field, δ 0.00 (q, 121 Hz). These effects are similar to but less pronounced than those found in the β-agostic complexes [Cp*Co(PR_3)Et][BF_4] (R = alkyl, aryl,[34] OMe[35]). In the ^{1}H NMR spectra the α-alkyl protons are found at high field (−0.3 to −0.7 ppm) as are the ethyl β-protons to a smaller extent (−0.05 ppm). The room-temperature NMR spectra do not give any additional information concerning the agostic behaviour of the alkyl groups.

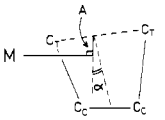

Figure 2. Geometrical parameters *A* and α used in the geometry optimization of the diene–metal bonding in CpZr(C_4H_6)Cl(·L).

Table IX. Optimized Values for the Geometrical Parameters *A* and α in the Model System CpZr(C_4H_6)Cl•L

L	*A*, Å	α, deg
none	0.13	17
NH_3	0.29	17
PH_3	0.28	19

The ^{1}H and ^{13}C NMR chemical shifts and the $^1J_{CH}$ coupling constants in the temperature-dependent spectra of the allyl (**13**) and 1-methallyl (**14**) complexes are in agreement with η^3-bound allylic ligands.[36]

Extended Hückel MO Calculations. To get an impression of the bonding in these complexes and to clarify the difference between the 16e and 14e complexes, we performed a series of extended Hückel MO calculations[37] on the model system CpZr(C_4H_6)Cl and its NH_3/PH_3 adducts. The coordination geometry of the diene fragment was optimized by minimizing the sum of one-electron energies for variations in the geometrical parameters *A* and α, depicted in Figure 2. This procedure was first used by Tatsumi et al. on $Cp_2Zr(C_4H_6)$ and $(CO)_3Fe(C_4H_6)$.[38] Geometrical parameters kept fixed in the calculations are found in the Experimental Section, together with the EH parameters used. Increasing *A* and/or decreasing α cor-

(34) (a) Brookhart, M.; Green, M. L. H.; Pardy, R. B. *J. Chem. Soc., Chem. Commun.* **1983**, 691. (b) Cracknell, R. B.; Orpen, A. G.; Spencer, J. L. *J. Chem. Soc., Chem. Commun.* **1984**, 326.

(35) Schmidt, G. F.; Brookhart, M. *J. Am. Chem. Soc.* **1985**, *107*, 1443.

(36) (a) Jolly, P. W.; Mynott, R. *Adv. Organomet. Chem.* **1981**, *19*, 257. (b) Benn, R.; Rufinska, A. *Organometallics* **1985**, *4*, 209.

(37) Hoffmann, R. *J. Chem. Phys.* **1963**, *39*, 1397.

(38) Tatsumi, K.; Yasuda, H.; Nakamura, A. *Isr. J. Chem.* **1983**, *23*, 145.

Table X. Calculated Mulliken Overlap Populations for $CpZr(C_4H_6)Cl \cdot L$

	L				
	none	NH_3[a]	PH_3[a]	$Cp_2Zr(cis\text{-}C_4H_6)$[b]	$CpTa(C_4H_6)Cl_2$[c]
$M-C_T$	0.349	0.329	0.301	0.338	0.298
$M-C_C$	0.089	0.116	0.096	0.060	0.108
C_C-C_T	0.962	0.948	0.977	0.991	0.956
C_C-C_C	1.038	1.036	1.020	1.012	1.037

[a] Overlap populations averaged for the nonidentical halves of the diene in the asymmetrical Lewis base adducts. [b] Values from ref 38. [c] Values from ref 4.

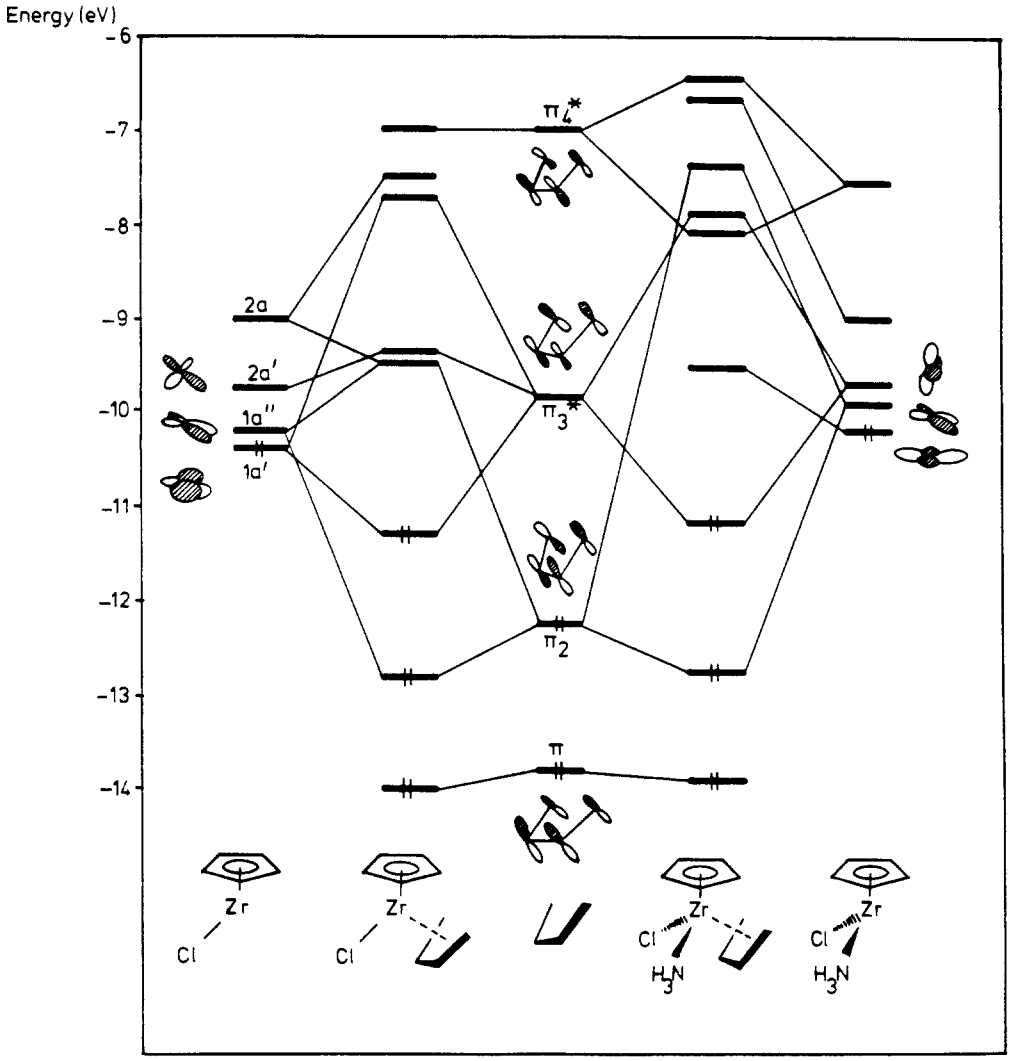

Figure 3. Orbital interaction diagrams for $CpZr(C_4H_6)Cl$ and its NH_3 adduct at optimized geometries.

responds to a decreasing contribution of the metallacyclopentene bonding structure. The optimized values of A and α (Table IX) show that on adding a Lewis base, the diene assumes a conformation with less metallacyclopentene character than in the 14e system. Furthermore, the availability of π-acceptor orbitals on the Lewis base does not influence the diene coordination geometry to a great extent: only a small increase in the metallacyclopentene character is observed.

From the calculated Mulliken overlap populations[39] (Table X) it can be seen that the terminal diene carbons interact more strongly with the metal than the internal diene carbons and that the internal C–C overlap populations are larger than those of the terminal C–C bonds. This indicates a metallacyclopentene-like bonding with inversion of the diene double bond–single bond pattern.

Differences between the 14e and 16e systems in the bonding of the diene are reflected in the MO interaction diagrams for the interaction between a *cis*-butadiene ligand and the fragments CpZrCl and $CpZrCl \cdot NH_3$ (Figure 3). The $CpZrCl \cdot NH_3$ frontier orbitals are very similar in sequence and character to those of the isoelectronic fragment $CpTaCl_2$[4] (but lacking its symmetry). Frontier orbitals of CpZrCl can be compared to the occupied orbitals 1a′ and 1a″ calculated for bent CpCoL.[40] The interaction of the occupied diene π_2 orbital with metal fragment is approximately the same in complexes with or without the Lewis base; on the other hand differences appear in the interaction of the unoccupied diene π_3* orbitals with the metal fragment. The $CpZrCl-\pi_3$* interaction is mainly due to the CpZrCl HOMO, which overlaps predominantly with methylene carbons of the diene. The $CpZrCl \cdot NH_3-\pi_3$*

(39) Mulliken, R. S. *J. Chem. Phys.* **1955**, *23*, 1833.

(40) Hofmann, P.; Padmanabhan, M. *Organometallics* **1983**, 2, 1273.

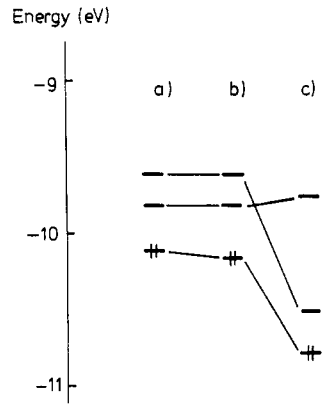

Figure 4. Frontier orbital energies for the fragments (a) $CpZrCl{\cdot}NH_3$, (b) $CpZrCl{\cdot}PH_3$ without P 3d orbitals, and (c) $CpZrCl{\cdot}PH_3$ with P 3d orbitals.

interaction is dominated by a strong mixing in of the $CpZrCl{\cdot}NH_3$ NLUMO (similar to the interaction in "supine" $CpTa(C_4H_6)Cl_2$[4]). This orbital has a lobe that is favorable for overlap with the internal diene carbons. These differences can be seen in the HOMO's of the diene complexes: calculated overlap populations within these MO's show that the Zr–central diene carbon overlap has more than doubled in the HOMO of the Lewis base adduct ($CpZr(C_4H_6)Cl$ HOMO, $P(Zr-C_T) = 0.218$, $P(Zr-C_C) = 0.031$; $CpZr(C_4H_6)Cl{\cdot}NH_3$ HOMO, $P(Zr-C_T) = 0.203$, $P(Zr-C_C) = 0.078$).

The availability of π-acceptor orbitals on the Lewis base does not change the overall composition of the CpZrCl·L frontier orbitals to a great extent, but it lowers the energy of the orbitals that interact with the diene π_3*, while the energy of the orbital interacting with the diene π_2 remains essentially unaffected (Figure 4). This increases the metal character in the metal fragment–diene π_3* bonding combination and changes the relative weighting of the participation of π_2 and π_3* in the diene complex. This will affect the C–C bonding within the butadiene ligand. Thus the C–C overlap populations in $CpZr(C_4H_6)Cl{\cdot}PH_3$ show less inversion of the butadiene single bond–double bond sequence than in the NH_3 adduct. This illustrates that the coordination geometry of the diene and the diene carbon–carbon distances are determined by separate effects: the first by spatial overlap and the second by the relative participation of π_2 and π_3* in the diene–metal bonding. That these effects can indeed be separated is supported by the observation of Yasuda et al. from a comparison of crystallographic data of many 1,3-diene–metal complexes, viz., that the relative C–C bond lengths in coordinated 1,3-dienes are not an accurate measure for the 1,4-σ-bond character.[4] Further investigation of these effects within the series of Cp*M(diene)Cl·L complexes by structure determinations will be difficult due to the high accuracy required. So far the calculations seem to support the conclusion from the NMR spectra that metallacyclopentene character is present in both 14e and 16e complexes but more pronounced in the 14e system.

X-ray Crystal Structure Determinations. The molecular structure of the 16e adduct $Cp^*Hf(C_6H_{10})Cl{\cdot}py$ was determined by single-crystal X-ray diffraction. The structure, shown in Figure 5 (interatomic distances and angles in Table XI), displays a cis-coordinated 2,3-dimethylbutadiene ligand in "supine" conformation, with a clear σ^2,π-metallacyclopentene character. The diene ligand shows the expected inversion of the C–C bond length sequence from that in the free diene: the internal C–C distance (C(17)–C(19)) is >0.1 Å shorter than each of the terminal C–C bonds (C(17)–C(18)/C(19)–C(20)). The

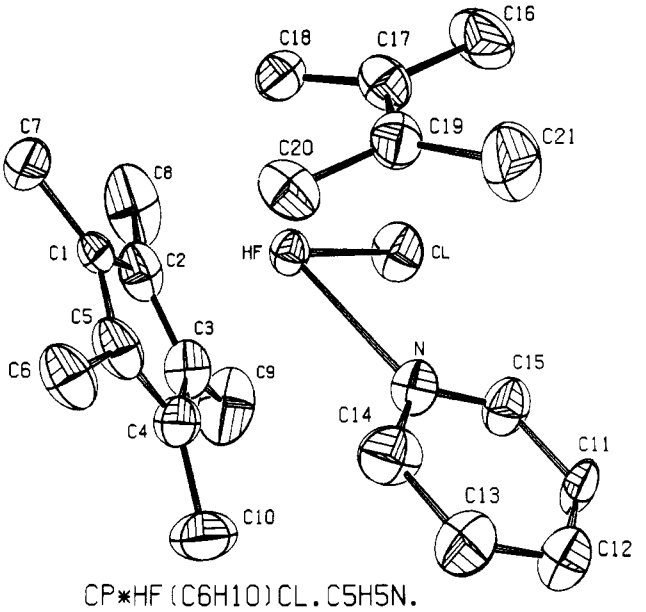

Figure 5. Molecular structure of $Cp^*Hf(C_6H_{10})Cl{\cdot}C_5H_5N$ (6·py), ORTEP representation. Thermal ellipsoids are drawn at the 50% probability level.

Table XI. Bond Distances (Å) and Angles (deg) for $Cp^*Hf(2,3\text{-dimethyl-}1,3\text{-butadiene})Cl \bullet C_5H_5N$ (6 • py) (Estimated Standard Deviations in Parentheses)

Bond Distances			
Hf–Cl	2.536 (2)	C(1)–C(7)	1.478 (13)
Hf–N	2.436 (7)	C(2)–C(8)	1.539 (13)
Hf–C(1)	2.532 (7)	C(3)–C(9)	1.495 (14)
Hf–C(2)	2.568 (9)	C(4)–C(10)	1.504 (14)
Hf–C(3)	2.652 (10)	C(5)–C(6)	1.525 (12)
Hf–C(4)	2.644 (10)	N–C(14)	1.365 (11)
Hf–C(5)	2.558 (8)	C(14)–C(13)	1.379 (13)
Hf–C(17)	2.483 (10)	C(13)–C(12)	1.387 (15)
Hf–C(18)	2.274 (10)	C(12)–C(11)	1.349 (15)
Hf–C(19)	2.477 (9)	C(11)–C(15)	1.375 (15)
Hf–C(20)	2.278 (10)	N–C(15)	1.363 (15)
C(1)–C(2)	1.471 (13)	C(17)–C(18)	1.493 (14)
C(2)–C(3)	1.482 (15)	C(19)–C(20)	1.513 (14)
C(3)–C(4)	1.432 (13)	C(17)–C(19)	1.384 (15)
C(4)–C(5)	1.502 (14)	C(16)–C(17)	1.531 (14)
C(5)–C(1)	1.458 (12)	C(19)–C(21)	1.56 (2)

Bond Angles			
Cl–Hf–N	83.8 (2)	C(1)–C(5)–C(6)	123.5 (9)
C(18)–Hf–C(20)	75.4 (6)	C(5)–C(1)–C(7)	125.6 (8)
Hf–C(18)–C(17)	79.5 (6)	C(2)–C(1)–C(7)	128.9 (8)
Hf–C(20)–C(19)	79 (1)	C(16)–C(17)–C(18)	122.6 (9)
C(1)–C(2)–C(3)	110.0 (8)	C(16)–C(17)–C(19)	119.0 (9)
C(2)–C(3)–C(4)	108.0 (8)	C(18)–C(17)–C(19)	118.3 (9)
C(3)–C(4)–C(5)	106.8 (8)	C(17)–C(19)–C(20)	117 (1)
C(4)–C(5)–C(1)	110.2 (8)	C(17)–C(19)–C(21)	126.0 (8)
C(5)–C(1)–C(2)	105.0 (9)	C(20)–C(19)–C(21)	117 (1)
C(1)–C(2)–C(8)	126.1 (9)	N–C(15)–C(11)	121 (1)
C(3)–C(2)–C(8)	123.8 (8)	C(15)–C(11)–C(12)	121 (1)
C(2)–C(3)–C(9)	123.0 (8)	C(11)–C(12)–C(13)	118.3 (9)
C(4)–C(3)–C(9)	128.7 (9)	C(12)–C(13)–C(14)	120 (1)
C(3)–C(4)–C(10)	125.4 (9)	C(13)–C(14)–N	122 (1)
C(5)–C(4)–C(10)	127.2 (8)	C(14)–N–C(15)	117.6 (9)
C(4)–C(5)–C(6)	125.8 (9)		

distances from Hf to the diene methylene carbon atoms (Hf–C(18) = 2.274 (10) Å, Hf–C(20) = 2.278 (10) Å) are similar to those found in $Cp_2Hf(2,3\text{-dimethyl-}1,3\text{-butadiene})$ (2.267 (5) Å).[33] Despite the asymmetry in the coordination sphere, the asymmetry in the diene Hf–C and C–C distances does not exceed 2σ. The σ^2,π-character is clearly shown by the fact that the diene methylene carbons are much closer to the metal than the internal diene carbons. The distance difference Δ = average $(M-C_C)$ – av-

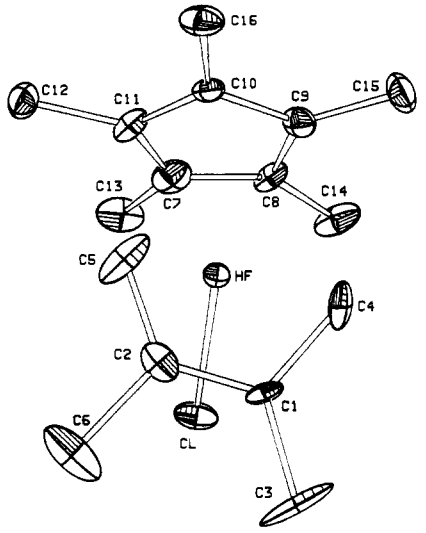

Figure 6. Molecular structure of $Cp^*Hf(C_6H_{10})Cl$ (**6**), ORTEP representation. Thermal ellipsoids are drawn at the 50% probability level.

erage ($M-C_T$) = 0.205 Å is much larger than in predominantly η^4-bonded diene complexes (where Δ is often negative, e.g., −0.08 Å in $(C_4H_6)Fe(CO)_3$[9] and −0.06 Å in $(C_4H_6)_2Mo(PMe_3)_2$[41]) but considerably smaller than in $Cp_2Hf(C_6H_{10})$ (Δ = 0.374 Å).[33] This reflects a larger contribution of the σ^2-bonding relative to the π-bonding in the metallocene derivatives, as visible in the ratio of the calculated M–C overlap populations: $P(M-C_T)/P(M-C_C)$ = 2.8 for $CpZr(C_4H_6)Cl\cdot NH_3$ and 5.6 for $Cp_2Zr(C_4H_6)$.[38]

An interesting feature in the structure of $Cp^*Hf(C_6H_{10})Cl\cdot py$ is the coordination of the Cp* ligand. The ring carbons C(3) and C(4) are 0.1 Å further away from the metal than the other three ring carbons, while essentially retaining the planarity of the ring. This suggests a partial slip of the Cp* ligand toward an η^3,π-type of bonding. This seems to be reflected in the Cp* ring C–C distances, with the shortest C–C bond (C(3)–C(4) = 1.43 Å) between the two carbons most distant from the metal and the two longest C–C bonds (C(4)–C(5) = 1.48 Å; C(2)–C(3) = 1.50 Å) between these carbons and the three-carbon part of the C_5 ring. Asymmetric bonding of cyclopentadienyl groups is not very common in transition-metal complexes. Significant distortions are found in complexes where a surplus of valence electrons is available, such as $(\eta^5\text{-Cp})(\eta^3\text{-Cp})Mo(CO)_2$[42] (in which the η^3-Cp ligand is also distinctly nonplanar) and $Cp_2Mn(PR_3)$[43] (with tilted, but planar Cp ligands). This is clearly not the reason for the distortion found in the electronically unsaturated 16e adduct here. The observation that the Cp* ring carbons most distant from the metal (C(3,4)), the Hf atom, and the central carbons of the butadiene ligand (C(17)–(19)) are very nearly in one plane suggests that a "trans-effect" phenomenon may cause the slight, but significant distortion from η^5-Cp* coordination in $Cp^*Hf(C_6H_{10})Cl\cdot py$. Interestingly, in the isoelectronic complex $CpTa(C_4H_6)Cl_2$[4] the Cp ligand is rotated 36° relative to the orientation in the Hf complex, no planar arrangement of four carbon atoms and the metal center is present, and no asymmetry in the Cp coordination is found. Recently a similar "trans-effect" distortion was reported for *cis*-$Cp^*Re(CO)_2I_2$.[44]

Table XII. Bond Distances (Å) and Angles (deg) for Cp^*Hf(2,3-dimethyl-1,3-butadiene)Cl (6) (Estimated Standard Deviations in Parentheses)

Bond Distances			
Hf–Cl	2.393 (2)	C(1)–C(2)	1.400 (12)
Hf–C(1)	2.478 (7)	C(1)–C(3)	1.47 (2)
Hf–C (2)	2.440 (8)	C(1)–C(4)	1.525 (13)
Hf–C(4)	2.236 (8)	C(2)–C(5)	1.397 (15)
Hf–C(5)	2.196 (10)	C(2)–C(6)	1.593 (15)
Hf–C(7)	2.495 (9)	C(7)–C(8)	1.396 (13)
Hf–C(8)	2.458 (8)	C(7)–C(11)	1.427 (12)
Hf–C(9)	2.447 (9)	C(8)–C(9)	1.477 (10)
Hf–C(10)	2.484 (8)	C(9)–C(10)	1.431 (12)
Hf–C(11)	2.504 (9)	C(10)–C(11)	1.405 (11)
Hf–CE[a]	2.158	C(7)–C(13)	1.497 (12)
		C(8)–C(14)	1.490 (12)
		C(9)–C(15)	1.493 (13)
		C(10)–C(16)	1.525 (11)
		C(11)–C(12)	1.511 (13)

Bond Angles			
Cl–Hf–CE[a]	114.55 (5)	C(7)–C(11)–C(10)	108.3 (8)
C(4)–Hf–C(5)	80.1 (3)	C(8)–C(7)–C(13)	124.0 (9)
C(2)–C(1)–C(3)	122.5 (9)	C(11)–C(7)–C(13)	127.0 (9)
C(2)–C(1)–C(4)	116.0 (7)	C(7)–C(8)–C(14)	127.2 (7)
C(3)–C(1)–C(4)	121.2 (8)	C(9)–C(8)–C(14)	124.9 (7)
C(1)–C(2)–C(5)	123.7 (9)	C(8)–C(9)–C(15)	128.7 (8)
C(1)–C(2)–C(6)	117.5 (8)	C(10)–C(9)–C(15)	125.2 (7)
C(5)–C(2)–C(6)	117.6 (9)	C(9)–C(10)–C(16)	123.7 (7)
C(8)–C(7)–C(11)	108.9 (7)	C(11)–C(10)–C(16)	127.1 (8)
C(7)–C(8)–C(9)	107.9 (7)	C(7)–C(11)–C(12)	125.6 (8)
C(8)–C(9)–C(10)	105.8 (7)	C(10)–C(11)–C(12)	125.8 (7)
C(9)–C(10)–C(11)	109.2 (6)		

[a] CE is centroid of Cp* ligand.

To make a final comparison between 14e and 16e complexes, an X-ray structure determination of Cp*Hf(2,3-dimethyl-1,3-butadiene)Cl (**6**) was carried out at 100 K. The structure is shown in Figure 6; bond lengths and angles are listed in Table XII. The compound is monomeric in the solid state, and the diene ligand is *s-cis* bound to the Hf atom. Remarkably the diene ligand shows a large asymmetry in the carbon–carbon distances, with one short internal C–C bond (C(1)–C(2) = 1.400 (12) Å) and one long and one short terminal C–C bond (C(1)–C(4) = 1.525 (13) Å and C(2)–C(5) = 1.397 (15) Å, respectively). This indicates an important contribution of the η^3,σ-resonance structure in the bonding of the diene molecule. Participation of η^3,σ-resonance structures has been suggested before for vinylketene complexes[45] but to our knowledge is unprecedented in complexes of symmetrical dienes. Interestingly, for the interconversion of (*s-trans*-η^4-conjugated diene)zirconocene complexes, a π-allyl–methylene intermediate was recently postulated by Erker et al.[46] The asymmetry in the 2,3-dimethyl-1,3-butadiene ligand might be induced by the electron deficiency of the metal atom. Asymmetry in ligand coordination due to interaction of an occupied ligand orbital with more than one empty metal orbital to obtain a more favorable overlap has been considered before in some theoretical studies.[47]

It is conceivable that an η^3,σ-coordinated diene ligand will have a low-energy fluxional process equivalencing the

(41) Brookhart, M.; Cox, K.; Cloke, F. G. N.; Green, J. C.; Green, M. L. H.; Hare, P. M.; Bashkin, J.; Derome, A. E.; Grebenik, P. D. *J. Chem. Soc., Dalton Trans.* **1985**, 423.
(42) Huttner, G.; Brintzinger, H. H.; Bell, L. G.; Friedrich, P.; Bejenke, V.; Neugebauer, D. *J. Organomet. Chem.* **1978**, *145*, 329.
(43) Howard, C. G.; Girolami, G. S.; Wilkinson, G.; Thornton-Pett, M.; Hursthouse, M. B. *J. Am. Chem. Soc.* **1984**, *106*, 2033.
(44) Einstein, F. W. B.; Klahn-Olivia, A. H.; Sutton, D.; Tyers, K. G. *Organometallics* **1986**, *5*, 53.
(45) Templeton, J. L.; Herric, R. S.; Rusic, C. A.; McKenna, C. E.; McDonald, J. W.; Newton, W. E. *Inorg. Chem.* **1985**, *24*, 1383.
(46) Erker, G.; Engel, K.; Korek, U.; Czisch, P.; Berke, H.; Caubere, P.; Vanderesse, R. *Organometallics* **1985**, *4*, 1531.
(47) (a) Lauher, J. W.; Hoffmann, R. *J. Am. Chem. Soc.* **1976**, *98*, 1739. (b) Goddard, R. J.; Hoffmann, R.; Jemmis, E. D. *Ibid.* **1980**, *102*, 7667. (c) Eisenstein, O.; Jean, Y. *Ibid.* **1985**, *107*, 1177.

two halves of the diene in solution NMR spectra.

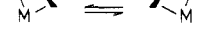

The average Hf–diene carbon distances determined from the X-ray structure show a distance difference [Δ = average (M–C_C) – average (M–C_T) = 0.243 Å] larger than that in the 16e pyridine adduct (Δ = 0.204 Å), as indicated by the EHMO calculations.[48]

Compounds **6** and **6**·py can be viewed to contain a hafnium atom in seven- and eight-coordination, respectively (counting Cp* to occupy three coordination sites). For Hf(IV) it is known that the effective ionic radius for eight-coordination is approximately 0.07 Å larger than for seven-coordination.[49] This is reasonably reflected in the average Hf–C(Cp*,C_T) distances in **6** and **6**·py: average Hf–C_T = 2.216 and 2.276 Å, average Hf–C(Cp*) = 2.482 and 2.553 Å, respectively (for **6**·py only the three Cp* carbon atoms closest to Hf are considered, vide supra). Though the Hf–Cl bond length in **6** (2.393 (2) Å) is quite normal for 14e seven-coordinate Hf complexes (e.g., $Cp^*HfCl_2[\eta^2\text{-}C(O)P(CMe_3)]_2$, Hf–Cl = 2.393/2.383 (2) Å[50]), the Hf–Cl bond in **6**·py is considerably longer than expected, >0.1 Å longer than in other 16e eight-coordinate Hf complexes (e.g., $(CH_2)_3(C_5H_4)_2HfCl_2$, Hf–Cl = 2.417 (3)/2.429 (2) Å[51]). This indicates a very unfavorable coordination geometry for Cl to Hf π-donation in **6**·py.

Concluding Remarks

The 14e diene complexes Cp*M(diene)X (M = Ti, Zr, Hf; X = Cl, alkyl, aryl) exhibit interesting features such as agostic C–H–M interactions in the alkyl derivatives and a significant participation of the η^3,σ-resonance structure in the bonding of the diene ligand. The influence of this bonding mode on the reactivity of the complexes is at present difficult to assess, as the main part of the reactivity studied so far involves initial adduct formation to give 16e species, in which the diene assumes a σ^2,π-metallacyclopentene structure. Reactions with polar unsaturated molecules such as CO,[11] RCN, RNC, and R_2CO give rise to a variety of products that all derive from initial insertion into the M–diene C_T bond. The compounds are also reactive toward unsaturated hydrocarbons. For instance, $Cp^*Hf(C_6H_{10})Me$ can catalyze the polymerization of ethylene and $Cp^*Hf(C_6H_{10})Cl$ reacts with acetylene to form an unusual, asymmetric 1,3-dihafnacyclobutane: $[Cp^*Hf(Cl)\text{-}\mu\text{-}CHCHCH_2C(Me)=C(Me)CH_2]_2$.[52] Full details of the reactivity of the complexes Cp*M(diene)X will be reported separately.

Experimental Section

General Considerations. All manipulations were carried out by using Schlenk or glovebox techniques under an atmosphere of purified dinitrogen. All solvents were distilled from Na/K alloy under dinitrogen. PMe_3[53] and PEt_3[54] were prepared according to published procedures. Other liquid reagents were purchased and were either distilled or vacuum transferred and stored over activated molecular sieves (4 Å). Cp^*TiCl_3[55] and $Cp^*M(C_4H_6)(C_4H_7)$[7b] (M = Ti, Zr, Hf) were prepared according to published procedures. Cp^*MCl_3 (M = Zr, Hf) was used as both prepared according to ref 7 and obtained through a synthesis in diethyl ether (a modification of the procedure in ref 56, described below). (2,3-Dimethyl-2-butene-1,4-diyl)Mg·2THF was prepared by a modification of published procedures[2b,57] and is described below. IR spectra were recorded on a JASCO IRA-2 or a Pye-Unicam SP3-300 spectrophotometer using Nujol mulls between KBr disks. ^1H NMR spectra were recorded at 60 MHz on a JEOL C-60 HL spectrometer and at 200 MHz with a Nicolet NT-200 spectrometer. ^{13}C NMR (50.3 MHz) and ^{31}P NMR (81.0 MHz) spectra were recorded on a Nicolet NT-200 spectrometer. GC analyses were performed on a Packard-Becker 428 gas chromatograph with a 25 m × 0.24 mm WCOT glass capillary column, coated with SE-30 (Chrompack). Melting points and decomposition temperatures were determined by differential thermal analysis (DTA), heating rate 2–3 °C/min. Elemental analyses were performed at the microanalytical department of the chemical laboratories, Groningen University, under supervision of Mr. A. F. Hamminga. All found percentages are the average of at least two independent determinations.

Preparation of Cp^*MCl_3 (M = Zr, Hf). A suspension of $HfCl_4$ (13.9 g, 43.3 mmol) and Cp*Li (6.5 g, 45.8 mmol) in 350 mL of diethyl ether was stirred for 4 days at room temperature. By then most of the solid had dissolved, yielding a greenish yellow solution. The solvent was pumped off, and the resultant yellow material was vacuum dried at 50 °C. For removal of residual complexed diethyl ether, the mixture was stirred with 80 mL of toluene at 70 °C for 30 min after which the toluene was pumped off. The solid was then washed twice with 30 mL of pentane and dried. Sublimation at 10^{-5} torr, using an IR lamp (Homef LB-01, 250 W, at 80–90 V), yielded pale greenish crystalline Cp^*HfCl_3 (13.7 g, 32.6 mmol, 75%). Anal. Calcd for $C_{10}H_{15}HfCl_3$: Hf, 42.49. Found: Hf, 42.84. The procedure for Cp^*ZrCl_3 is similar, but 2–3 days of reaction time was sufficient; yield 70%. Anal. Calcd for $C_{10}H_{15}ZrCl_3$: C, 36.09; H, 4.54; Zr, 27.41; Cl, 31.96. Found: C, 36.17; H, 4.70; Zr, 27.62; Cl, 31.96.

Preparation and Use of (2,3-Dimethyl-2-butene-1,4-diyl)Mg·2THF. For the synthesis of $(C_6H_{10})Mg\cdot 2THF$ magnesium was activated by adding either 0.3 mL of PhI or 1 mL of leftover THF solution of $(C_6H_{10})Mg\cdot 2THF$ to Mg turnings in THF with free 2,3-dimethyl-1,3-butadiene present and shaking this mixture for 2 days at room temperature. Shaking this activated Mg in THF, to which 2,3-dimethyl-1,3-butadiene was added, for 4 days at room temperature produced an orange-yellow solution that was decanted and filtered. The liquid was then vacuum transferred to be used again for subsequent batches. The resultant orange oil was not pumped dry[58] but redissolved in THF. The solution was calibrated and used as a Grignard solution (typical molarity: 0.2–0.3 M).

Preparation of $Cp^*M(C_5H_8)Cl$ (M = Zr, 2; M = Hf, 5). A solution of Cp^*HfCl_3 (8.6 g, 20.5 mmol) and 2-methyl-1,3-butadiene (3.1 mL, 31.0 mmol) in 100 mL of THF was stirred with a 4-fold excess of 1% Na/Hg for 24 h at room temperature. Subsequently the THF was pumped off and the resultant brown-yellow solid extracted with hot toluene. Concentration and cooling of the toluene solution to −30 °C gave yellow-brown crystals of **5** (7.1 g, 17.0 mmol, 83%): IR 2725 (vw), 1530 (w), 1483 (mw), 1398 (mw), 1375 (m), 1315 (vw), 1215 (w), 1110 (w), 1064 (vw), 1023 (m), 983 (mw), 968 (vw), 908 (w), 850 (m), 834 (w), 804 (s), 723 (vw), 611 (mw), 539 (vw), 545 (w), 523 (w), 468 (mw) cm^{-1}. **2** was prepared analogously with the appropriate reagents. The yield, however, was much lower (15%). Elemental analyses of **2** and **5** can be found in ref 11.

(48) Although the calculations performed only pertain to symmetrical diene systems, it is probable that the optimum symmetrical geometry and the symmetrical average of the η^3,σ-structure are reasonably similar, as the interconversion of the η^3,σ-configurations appears to have a very low-energy barrier and is likely to follow a path of least motion.

(49) Shannon, R. D. *Acta Crystallogr., Sect. A: Cryst. Phys., Diffr., Theor. Gen. Crystallogr.* **1976**, *A32*, 751.

(50) Roddick, D. M.; Santarsiero, B. D.; Bercaw, J. E. *J. Am. Chem. Soc.* **1985**, *107*, 4670.

(51) Saldarriaga-Molina, C. H.; Clearfield, A.; Bernal, I. *Inorg. Chem.* **1974**, *13*, 2880.

(52) Hessen, B.; Van Bolhuis, F.; Teuben, J. H., in preparation.

(53) Basolo, F. *Inorganic Synthesis*; McGraw-Hill: New York, 1976; Vol. XVI, p 153.

(54) Hewitt, F.; Holliday, A. K. *J. Chem. Soc.* **1953**, 530.

(55) Bercaw, J. E.; Marvich, R. H.; Bell, L. G.; Brintzinger, H. H. *J. Am. Chem. Soc.* **1972**, *94*, 1219.

(56) Wengrovius, J. H.; Schrock, R. R. *J. Organomet. Chem.* **1981**, *205*, 319.

(57) (a) Fujita, K.; Ohnuma, Y.; Yasuda, H.; Tani, H. *J. Organomet. Chem.* **1976**, *113*, 201. (b) Yasuda, H.; Nakano, H.; Natsukawa, K.; Tani, H. *Macromolecules* **1978**, *11*, 586.

(58) When the yellow-orange oil was dried in vacuo at 40 °C, a yellow pyrophoric solid was obtained, which upon redissolving in THF gave a yellow solution and a greenish precipitate of metallic Mg. This causes unwanted reduction side reactions in the reaction with Cp^*TiCl_3.

Preparation of Cp*M(C_6H_{10})Cl (M = Zr, 3; M = Hf, 6). A solution of Cp*$HfCl_3$ (8.8 g, 21.0 mmol) and 2,3-dimethyl-1,3-butadiene in 100 mL of THF was stirred with a 4-fold excess of 1% Na/Hg for 24 h at room temperature. Subsequently the THF was pumped off and the resultant brown solid extracted with pentane. Evaporation of the pentane yielded the crude brown THF adduct. Sublimation (115 °C, 10^{-3} torr) gave yellow **6** (5.6 g, 13.0 mmol, 62%): IR 2732 (vw), 1521 (br w), 1485 (mw), 1408 (mw), 1375 (m), 1285 (w), 1174 (m), 1066 (vw), 1025 (m), 981 (w), 900 (vw), 855 (s), 832 (vw), 802 (w), 715 (mw), 621 (w), 531 (mw), 480 (m) cm^{-1}. The corresponding Zr compound **3** was prepared analogously. However, during sublimation (100 °C, 10^{-3} torr) *partial decomposition of the compound occurred, lowering the* yield (20%). **3**: mol wt calcd, 344; mol wt found, 333 (cryoscopy in benzene). Elemental analyses for **3** and **6** can be found in ref 11.

Preparation of Cp*Ti(C_6H_{10})Cl (7). Into a solution of Cp*$TiCl_3$ (1.12 g, 3.88 mmol) in 30 mL of THF at 0 °C was syringed 15 mL of a 0.26 M solution of (C_6H_{10})Mg in THF dropwise in 50 min. After the resultant brown-green solution was stirred at room temperature for 15 h, the THF was pumped off and residual THF removed by pumping off 5 mL of pentane. Extracting the mixture twice with 30 mL of pentane and cooling the concentrated extracts to −80 °C yielded, after the product was washed twice with very cold pentane, blue-green crystalline **7** (0.44 g, 1.46 mmol, 37%): IR 3030 (w), 2720 (vw), 1653 (vw), 1488 (m), 1430 (m), 1422 (m), 1378 (s), 1210 (mw), 1182 (mw), 1065 (vw), 1025 (m), 1002 (w), 830 (m), 804 (vw), 732 (mw), 613 (vw), 520 (w), 506 (mw), 479 (m), 405 (s), 394 (sh) cm^{-1}. Anal. Calcd for $C_{16}H_{25}TiCl$: C, 63.90; H, 8.38; Ti, 15.93; Cl, 11.79. Found: C, 63.51; H, 8.42; Ti, 15.80; Cl, 11.78.

Ligand Exchange between Cp*M(C_4H_6)(C_4H_7) and Cp*MCl_3 (M = Zr, Hf). Cp*$ZrCl_3$ (0.95 g, 2.85 mmol) was extracted into 130 mL of diethyl ether. Cp*Zr(C_4H_6)(C_4H_7) (0.97 g, 2.89 mmol) was added and dissolved by stirring briefly. The resultant deep red solution was allowed to stand at room temperature for 4 days, during which small purple crystals precipitated. The liquid was filtered off, and the product was washed twice with diethyl ether and dried, yielding **1** (0.73 g, 2.32 mmol, 81%): IR 3050 (w), 3020 (w), 2720 (vw), 1500 (sh), 1688 (mw), 1628 (w), 1617 (mw), 1477 (m), 1208 (mw), 1149 (mw), 1120 (vw), 1066 (vw), 1030 (m), 1025 (sh), 939 (w), 850 (w), 815 (w), 795 (s), 678 (vw), 535 (vw), 443 (mw), 380 (mw) cm^{-1}. Anal. Calcd for $C_{14}H_{21}ZrCl$: C, 53.21; H, 6.70; Zr, 28.87; Cl, 11.22. Found: C, 52.95; H, 6.69; Zr, 28.82; Cl, 11.22. The solvent of the mother liquor was pumped off, and the orange residue was washed with 10 mL of pentane. The yellow solid was then extracted with 45 mL of diethyl ether. Cooling the extract to −80 °C yielded bright yellow Cp*Zr(C_4H_7)Cl_2 (0.31 g, 0.89 mmol, 31%): IR 2725 (vw), 1562 (mw), 1483 (m), 1432 (m), 1420 (sh), 1381 (s), 1304 (vw), 1272 (vw), 1182 (mw), 1113 (vw), 1065 (vw), 1028 (s), 982 (w), 883 (vw), 859 (m), 800 (vw), 788 (m), 660 (mw), 522 (mw), 431 (mw) cm^{-1}. Anal. Calcd for $C_{14}H_{22}ZrCl_2$: C, 47.71; H, 6.29; Cl, 20.12. Found: C, 47.63; H, 6.22; Cl, 20.17. For M = Hf a similar procedure yielded $Cp^*_2Hf_2(C_4H_6)Cl_4$ (yield 75%) as orange-brown crystals in 15 h at room temperature. Anal. Calcd for $C_{26}H_{36}Hf_2Cl_4$: C, 35.01; H, 4.41; Cl, 17.22. Found: C, 35.27; H, 4.50; Cl, 16.98. From the mother liquor yellow Cp*Hf(C_4H_7)Cl_2 was isolated. Anal. Calcd for $C_{14}H_{22}HfCl_2$: C, 38.24; H, 5.04; Cl, 16.12. Found: C, 38.34; H, 5.19; Cl, 16.10.

Preparation of Cp*M(C_6H_{10})R (8–14). **6** (2.60 g, 6.03 mmol) was dissolved in 20 mL of diethyl ether. At −30 °C 10 mL of an 0.60 M solution of $(CH_3)_3CCH_2MgCl$ in diethyl ether was syringed in dropwise. After the solution was stirred for 5 h while being warmed up to room temperature, the solvent was pumped off and the resultant yellow solid was extracted with pentane. Crystallization from pentane yielded yellow crystalline **11** (2.30 g, 4.93 mmol, 81%): IR 2720 (vw), 1492 (mw), 1440 (m), 1406 (w), 1388 (mw), 1356 (m), 1282 (w), 1216 (m), 1170 (mw), 1097 (w), 1030 (m), 1010 (vw), 988 (w), 930 (vw), 915 (vw), 893 (w), 865 (s), 807 (mw), 780 (m, br), 755 (mw), 716 (w), 618 (mw), 553 (w), 500 (w), 480 (w) cm^{-1}. Anal. Calcd for $C_{21}H_{36}Hf$: C, 54.01; H, 7.77; Hf, 38.22. Found: C, 53.99; H, 7.79; Hf, 38.01. The other hydrocarbon derivatives could be prepared similarly by using the appropriate Grignard or alkyllithium reagents. The methyl and ethyl complexes were kept at or below 0 °C while in solution. All compounds were obtained in 70–80% yields and gave satisfactory elemental analyses (supplementary material).

Preparation of Cp*Hf(C_6H_{10})BH_4. **6** (0.99 g, 2.29 mmol) and $NaBH_4$ (0.29 g, 7.6 mmol) were stirred together in 20 mL of diethyl ether for 2 days at room temperature. The solid material was allowed to settle, and the clear red-orange solution was filtered. Concentrating and cooling the solution to −80 °C yielded deep orange-red crystals of Cp*Hf(C_6H_{10})BH_4 (0.77 g, 1.87 mmol, 81%): ^1H NMR (200 MHz, C_6D_6, 20 °C) 1.94 (s, 15 H, Cp*), 2.25 (s, 6 H, CH_3), 1.83 (d, 2 H, 10.2 Hz, *syn*-CH_2), −0.22 (d, 2 H, 10.2 Hz, *anti*-CH_2), 1.4 ppm (br q, J_{BH} = 76 Hz, BH_4). IR: 2725 (vw), 2450 (m), 2410 (s), 2225 (vw), 2100 (mw), 2025 (mw), 1965 (br m), 1484 (mw), 1378 (s), 1290 (vw), 1179 (mw), 1121 (m), 1065 (vw), 1022 (mw), 985 (vw), 900 (w), 848 (s), 802 (vw), 718 (w), 620 (mw), 540 (w), 496 (mw), 422 (mw) cm^{-1}. Anal. Calcd for $C_{16}H_{19}BHf$: C, 46.79; H, 7.12. Found: C, 47.04; H, 6.99.

Preparation of Cp*Hf(C_6H_{10})Cl·PMe_3 and Other Lewis Base Adducts of 3 and 6. To a solution of **6** (0.54 g, 1.3 mmol) in 15 mL of diethyl ether was added a small excess of PMe_3. While being stirred for 30 min at room temperature, the solution turned from orange to brown. Subsequently the solvent and excess of PMe_3 were pumped off, and the brown solid was recrystallized from pentane. Cp*Hf(C_6H_{10})Cl·PMe_3 (0.58 g, 1.15 mmol, 90%) was isolated. Anal. Calcd for $C_{19}H_{34}HfClP$: C, 44.98; H, 6.75; Cl, 6.99. Found: C, 45.14; H, 6.88; Cl, 7.01. The other adducts were prepared similarly, except for the pyridine and 2,6-xylyl cyanide adducts of **6**, which are only sparingly soluble in pentane. They were precipitated from pentane or recrystallized from diethyl ether. The 2,6-xylyl cyanide adduct of **6** was always kept at 0 °C to prevent further reaction.[20] All compounds were obtained in 70–90% yield and gave satisfactory elemental analyses (supplementary material).

Reaction of Cp*M(diene)Cl (2, 3, 5, 6) with Dry Oxygen. A solution of **6** in 5 mL of pentane was stirred under an excess of dry oxygen for 1 h at room temperature. Immediately after the admission of O_2 a white solid precipitated. The volatile products were collected in a cold trap (−196 °C). The liquid was shown by GC (using 2,3-dimethyl-1,3-butadiene as standard) to contain 2.1 mmol (0.95 mmol/mmol of Hf) of 2,3-dimethyl-1,3-butadiene. Using the same procedure the compounds **2**, **3**, and **5** were shown to produce 0.85–0.95 mmol/mmol of Zr (or Hf) of the free diene upon reaction with dry oxygen.

Molecular Orbital Calculations. Calculations were of the extended Hückel type[37,59] with weighted H_{ij}'s.[60] H_{ij}'s for Zr were obtained from a charge-iterative calculation on the bent CpZr(C_4H_6) fragment with quadratic charge dependence on Zr, using VSIE parameters from ref 61. The extended Hückel parameters H_{ij} used are (in eV): Zr 4d, −10.43; Zr 5s, −9.97; Zr 5p, −6.38; P 3s, −18.60; P 3p, −14.00; P 3d, −7.00; N 2s, −26.00; N 2p, −13.40; Cl 3s, −30.00; Cl 3p, −15.00; C 2s, −21.40; C 2p, −11.40 H 1s, −13.60. The Slater orbital exponents for Zr were taken from ref 38. Used Slater orbital exponents: Zr 4d, 3.835 (0.6211) + 1.505 (0.5796); Zr 5s, 1.776; Zr 5p, 1.817; P 3s, 3p, 1.600; P 3d, 1.400; N 2s, 2p, 1.950; Cl 3s, 3p, 2.033; C 2s, 2p, 1.625; H 1s, 1.300. Geometrical parameters not stated in the text include the following: Zr–Cl, 2.50 Å; Zr–Cp(centroid), 2.56 Å; Zr–N, 2.40 Å; Zr–P, 2.56 Å; Zr–C(butadiene), 2.32 Å (at L = 0, α = 0); C–C(butadiene), 1.44 Å; C–H, 1.09 Å; P–H, 1.40 Å; N–H, 1.05 Å; C–C–C(butadiene), 120°; Cl–Zr–X (X = N and P in the Lewis base adducts), 82°; Cp(centroid)–Zr–Cl (in 14e complex), 120°.

X-ray Structure Determinations. Crystallographic Data. X-ray diffraction on **6** and **6**·py was carried out on an Enraf-Nonius CAD-4D diffractometer, interfaced to a PDP-11/23, with graphite-monochromatized Mo Kα radiation. Relevant crystallographic data can be found in Table XIII.

Collection and Reduction of Intensity Data. Crystals suitable for X-ray diffraction were obtained for **6**·py by diffusion of pentane into a toluene solution of the compound at room

(59) A Fortran 5 version of the program ICON 8 (Howell, J.; Rossi, A.; Wallace, D.; Haraki, K.; Hoffmann, R. Cornell University, Ithaca, NY) was used (QCPE 469).

(60) Ammeter, J. H.; Bürgi, H. B.; Thibeault, J. C.; Hoffmann, R. *J. Am. Chem. Soc.* **1978**, *100*, 3686.

(61) Baranovskii, V. L.; Nikol'skii, A. B. *Theor. Exp. Chem. (Engl. Transl.)* **1967**, *3*, 309.

Table XIII. Crystallographic Data for $Cp^*Hf(C_6H_{10})Cl \cdot py$ and $Cp^*Hf(C_6H_{10})Cl$

formula	$C_{21}H_{30}HfClN$	$C_{16}H_{25}HfCl$
mol wt	510.4	431.3
space group	$Pna2_1$	C_2
a, Å	17.412 (3)	8.820 (3)
b, Å	8.164 (3)	12.767 (3)
c, Å	14.837 (3)	14.486 (3)
α, deg	90.0	90.0
β, deg	90.0	102.59 (1)
γ, deg	90.0	90.0
V, Å^3	2109.1	1592.1
Z	4	4
D_{calcd}, g cm^{-3}	1.607	1.799
μ, cm^{-1}	50.3	66.5
$F(000)$, e	504	840
T, K	293	100
cryst dimens, mm	0.10 × 0.27 × 0.50	0.45 × 0.49 × 0.106
radiation	Mo Kα	Mo Kα
scan mode	ω–2θ	ω–2θ
θ range, deg	1.0–27.0	1.0–38.0
hkl range	22,10,18	15,22,±25
std refl	$\bar{8}\bar{4}2$	$1\bar{1}7,\bar{1}36,620$
refl measd	2391	4457
refl obsd	2025 ($I \geq 2\sigma(I)$)	4010 ($I \geq 3\sigma(I)$)
no. of parameters refined	216	164
R	0.036	0.036
R_w ($w = 1$)	0.059	0.049

temperature and for **6** by slowly cooling a pentane solution to −30 °C. A crystal of **6**·py was sealed under dinitrogen in a thin-walled glass capillary. A crystal of **6** was mounted on a goniometer head under dinitrogen and then placed on the diffractometer in a stream of dinitrogen of 100 K. From systematic absences on Weissenberg films the space group of **6**·py was found to be $Pna2_1$ and of **6** was found to be $C2$, Cm, or $C2/m$. In the final state, group $C2$ gave the best fit. The Bragg angles of 24 reflections, with 12° < θ ≤ 15° and 10° ≤ θ ≤ 25° for **6**·py and **6**, respectively, were used to obtain the orientation matrix for the intensity data collection and to refine the unit cell parameters. Intensity data were collected by θ–2θ scans, with all reflections measured at the same scan speed. The ω scan width was given by (1.3 + 0.35 tan θ)° and (0.8 + 0.35 tan θ)° and the horizontal opening of the detector by (3.4 + 1.0 tan θ)° and (3.2 + 1.0 tan θ)° for **6**·py and **6**, respectively. Measuring time background to peak ratio is 1:2. Intensity standard reflections were used during data collection and inspected every 6000 s (fluctuation < 1–2%). The intensities were corrected for Lorentz and polarization effects and absorption (transmission coefficients from 0.601 to 0.269 for **6**·py and from 0.508 to 0.106 for **6**).

Determination and Refinement of the Structures. For **6**·py the Hf atom was located by Patterson synthesis: for **6** the Hf and Cl atoms were found by direct methods (MULTAN 82). The other non-hydrogen atoms were revealed from succeeding difference maps. Attempts to localize the hydrogen atoms from the final difference maps failed. Using anisotropic temperature factors, a full-matrix least squares of F converged for **6**·py to a final R = 0.036 and R_w = 0.059 (w = 1) and for **6** to a final R = 0.036 and R_w = 0.049 (w = 1). All calculations were performed by using CAD4-SDP programs.

Acknowledgment. We thank Professors K. Tatsumi and G. Erker for stimulating discussions. This investigation was supported by the Netherlands Foundation for Chemical Research (SON) with financial aid from the Netherlands Organization for the Advancement of Pure Research (ZWO).

Supplementary Material Available: Tables of elemental analyses of **8**–**14** and Cp*M(diene)Cl·L complexes and positional and thermal parameters and least-squares planes for **6** and **6**·py (8 pages); listings of observed and calculated structure factors for **6** and **6**·py (32 pages). Ordering information is given on any current masthead page.

Hydrido Silyl Complexes. 9.[1] Cr,H,Si Three-Center Bonding in $C_6Me_6(CO)_2Cr(H)SiHPh_2$

Ulrich Schubert,*[†] Johannes Müller,[†] and Helmut G. Alt[‡]

Institut für Anorganische Chemie der Universität Würzburg, Am Hubland, D-8700 Würzburg, West Germany, and Laboratorium für Anorganische Chemie der Universität Bayreuth, D-8580 Bayreuth, West Germany

Received July 14, 1986

$C_6Me_6(CO)_2Cr(H)SiHPh_2$ (**1**) contains a Cr,H,Si two-electron three-center bond in its ground state. Comparison of structural and ^{29}Si NMR data with those of the isoelectronic complex $C_5Me_5(CO)_2Mn(H)SiHPh_2$ (**2**) suggests that Si–H interaction in **1** is slightly stronger than in **2**. This is attributed to the increased size of the C_6Me_6 ligand. **1** crystallizes in the monoclinic space group $P2_1/n$ with a = 9.285 (7) Å, b = 15.86 (2) Å, c = 16.05 (2) Å, and β = 94.20 (7)° (Z = 4). Important bond lengths are Cr–Si = 2.456 (1), Cr–H = 1.61 (4), Si–H (bridging) = 1.61 (4), and Si–H (terminal) = 1.39 (3) Å. The Si,Cr,H coupling constant is 70.8 Hz.

Introduction

Complexes containing both a hydride and a silyl ligand, which are formed by oxidative addition of Si–H bonds to transition metals, are important intermediates in metal-catalyzed hydrosilylation reactions.[2] Substantial information on the factors governing these reactions can be obtained from the investigation of metal complexes containing metal–hydrogen–silicon three-center bonds in their ground states. Manganese complexes of the type (η^5-C_5R_5)(CO)(L)Mn(H)SiR_3 (L = CO, PR_3, $P(OR)_3$, CNR) are particularly well investigated in this respect; the results have been summarized in the introduction of ref 3.

[†] University of Würzburg.
[‡] University of Bayreuth.

(1) Part 8 in this series: Knorr, M.; Schubert, U. *Transition Met. Chem. (Weinheim, Ger.)* **1986**, *11*, 268.
(2) Speier, J. L. *Adv. Organomet. Chem.* **1977**, *17*, 407 and references cited therein.
(3) Schubert, U.; Scholz, G.; Müller, J.; Ackermann, K.; Wörle, B.; Stansfield, R. F. D. *J. Organomet. Chem.* **1986**, *306*, 303 and references cited therein.

0276-7333/87/2306-0469$01.50/0